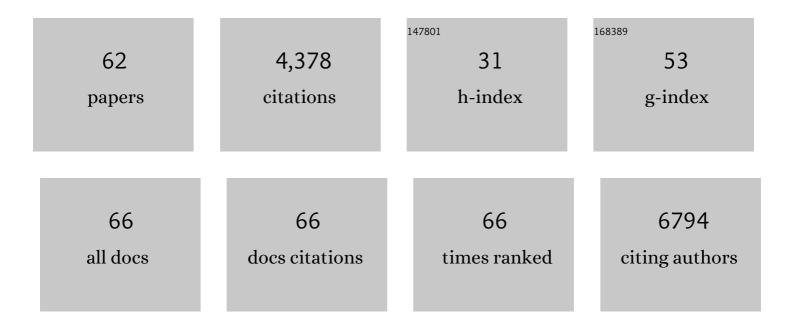
William R Crum

List of Publications by Year in descending order

Source: https://exaly.com/author-pdf/2092800/publications.pdf Version: 2024-02-01



#	Article	IF	CITATIONS
1	Patterns of temporal lobe atrophy in semantic dementia and Alzheimer's disease. Annals of Neurology, 2001, 49, 433-442.	5.3	641
2	Generalized Overlap Measures for Evaluation and Validation in Medical Image Analysis. IEEE Transactions on Medical Imaging, 2006, 25, 1451-1461.	8.9	583
3	Imaging of onset and progression of Alzheimer's disease with voxel-compression mapping of serial magnetic resonance images. Lancet, The, 2001, 358, 201-205.	13.7	414
4	Automatic Differentiation of Anatomical Patterns in the Human Brain: Validation with Studies of Degenerative Dementias. Neurolmage, 2002, 17, 29-46.	4.2	399
5	An evaluation of four automatic methods of segmenting the subcortical structures in the brain. NeuroImage, 2009, 47, 1435-1447.	4.2	180
6	Zen and the art of medical image registration: correspondence, homology, and quality. NeuroImage, 2003, 20, 1425-1437.	4.2	159
7	Progressive ventricular enlargement in patients with clinically isolated syndromes is associated with the early development of multiple sclerosis. Journal of Neurology, Neurosurgery and Psychiatry, 2002, 73, 141-147.	1.9	138
8	Implantation Site and Lesion Topology Determine Efficacy of a Human Neural Stem Cell Line in a Rat Model of Chronic Stroke. Stem Cells, 2012, 30, 785-796.	3.2	135
9	Automated Hippocampal Segmentation by Regional Fluid Registration of Serial MRI: Validation and Application in Alzheimer's Disease. NeuroImage, 2001, 13, 847-855.	4.2	124
10	Contrasting Effects of Haloperidol and Lithium on Rodent Brain Structure: A Magnetic Resonance Imaging Study with Postmortem Confirmation. Biological Psychiatry, 2012, 71, 855-863.	1.3	113
11	Correlations Between Apolipoprotein E ε4 Gene Dose and Whole Brain Atrophy Rates. American Journal of Psychiatry, 2007, 164, 916-921.	7.2	104
12	A comprehensive testing protocol for MRI neuroanatomical segmentation techniques: Evaluation of a novel lateral ventricle segmentation method. NeuroImage, 2011, 58, 1051-1059.	4.2	102
13	Reduced Cortical Volume and Elevated Astrocyte Density in Rats Chronically Treated With Antipsychotic Drugs—Linking Magnetic Resonance Imaging Findings to Cellular Pathology. Biological Psychiatry, 2014, 75, 982-990.	1.3	85
14	Reproducibility of thalamic segmentation based on probabilistic tractography. NeuroImage, 2010, 52, 69-85.	4.2	77
15	Changes in Neurocognitive Architecture in Patients with Obstructive Sleep Apnea Treated with Continuous Positive Airway Pressure. EBioMedicine, 2016, 7, 221-229.	6.1	68
16	Evolution of structural abnormalities in the rat brain following in utero exposure to maternal immune activation: A longitudinal in vivo MRI study. Brain, Behavior, and Immunity, 2017, 63, 50-59.	4.1	64
17	Performance characterization in computer vision: A guide to best practices. Computer Vision and Image Understanding, 2008, 109, 305-334.	4.7	53
18	Hippocampal Hypertrophy and Sleep Apnea: A Role for the Ischemic Preconditioning?. PLoS ONE, 2013, 8, e83173.	2.5	53

#	Article	IF	CITATIONS
19	An automated algorithm for the computation of brain volume change from sequential MRIs using an iterative principal component analysis and its evaluation for the assessment of whole-brain atrophy rates in patients with probable Alzheimer's disease. NeuroImage, 2004, 22, 134-143.	4.2	48
20	Segmentation of the thalamus in MRI based on T1 and T2. NeuroImage, 2011, 56, 939-950.	4.2	48
21	Neurorestoration induced by the <scp>HDAC</scp> inhibitor sodium valproate in the lactacystin model of <scp>P</scp> arkinson's is associated with histone acetylation and upâ€regulation of neurotrophic factors. British Journal of Pharmacology, 2015, 172, 4200-4215.	5.4	46
22	Test–retest reliability and longitudinal analysis of automated hippocampal subregion volumes in healthy ageing and <scp>A</scp> lzheimer's disease populations. Human Brain Mapping, 2018, 39, 1743-1754.	3.6	45
23	Evolution of Extra-Nigral Damage Predicts Behavioural Deficits in a Rat Proteasome Inhibitor Model of Parkinson's Disease. PLoS ONE, 2011, 6, e17269.	2.5	44
24	Dissociation between iron accumulation and ferritin upregulation in the aged substantia nigra: attenuation by dietary restriction. Aging, 2016, 8, 2488-2508.	3.1	43
25	Comparison and Evaluation of Segmentation Techniques for Subcortical Structures in Brain MRI. Lecture Notes in Computer Science, 2008, 11, 409-416.	1.3	40
26	Correlations of Behavioral Deficits with Brain Pathology Assessed through Longitudinal MRI and Histopathology in the R6/1 Mouse Model of Huntington's Disease. PLoS ONE, 2013, 8, e84726.	2.5	39
27	Mitochondrial displacements in response to nanomechanical forces. Journal of Molecular Recognition, 2008, 21, 30-36.	2.1	35
28	3D reconstruction of 2D fluorescence histology images and registration with in vivo MR images: Application in a rodent stroke model. Journal of Neuroscience Methods, 2013, 219, 27-40.	2.5	35
29	A New Validation Method for X-ray Mammogram Registration Algorithms Using a Projection Model of Breast X-ray Compression. IEEE Transactions on Medical Imaging, 2007, 26, 1190-1200.	8.9	34
30	Phenomenological Model of Diffuse Global and Regional Atrophy Using Finite-Element Methods. IEEE Transactions on Medical Imaging, 2006, 25, 1417-1430.	8.9	32
31	Accuracy assessment of global and local atrophy measurement techniques with realistic simulated longitudinal Alzheimer's disease images. NeuroImage, 2008, 42, 696-709.	4.2	32
32	Diamagnetic chemical exchange saturation transfer (diaCEST) affords magnetic resonance imaging of extracellular matrix hydrogel implantation in a rat model of stroke. Biomaterials, 2017, 113, 176-190.	11.4	29
33	Simultaneous effects on parvalbumin-positive interneuron and dopaminergic system development in a transgenic rat model for sporadic schizophrenia. Scientific Reports, 2016, 6, 34946.	3.3	27
34	Generalised Overlap Measures for Assessment of Pairwise and Groupwise Image Registration and Segmentation. Lecture Notes in Computer Science, 2005, 8, 99-106.	1.3	26
35	A Framework for Detailed Objective Comparison of Non-rigid Registration Algorithms in Neuroimaging. Lecture Notes in Computer Science, 2004, , 679-686.	1.3	25
36	Bringing memory fMRI to the clinic: Comparison of seven memory fMRI protocols in temporal lobe epilepsy. Human Brain Mapping, 2015, 36, 1595-1608.	3.6	22

WILLIAM R CRUM

#	Article	IF	CITATIONS
37	Information Theoretic Similarity Measures in Non-rigid Registration. Lecture Notes in Computer Science, 2003, 18, 378-387.	1.3	21
38	Simulation of two-dimensional tagged MRI. Journal of Magnetic Resonance Imaging, 1997, 7, 416-424.	3.4	20
39	Free-breathing radial acquisitions of the heart. Magnetic Resonance in Medicine, 2004, 52, 1127-1135.	3.0	20
40	Frequency-domain simulation of MR tagging. Journal of Magnetic Resonance Imaging, 1998, 8, 1040-1050.	3.4	17
41	A comparison of automated anatomical–behavioural mapping methods in a rodent model of stroke. Journal of Neuroscience Methods, 2013, 218, 170-183.	2.5	17
42	Correlations of Behavioral Deficits with Brain Pathology Assessed through Longitudinal MRI and Histopathology in the HdhQ150/Q150 Mouse Model of Huntington's Disease. PLoS ONE, 2017, 12, e0168556.	2.5	17
43	Registration of challenging pre-clinical brain images. Journal of Neuroscience Methods, 2013, 216, 62-77.	2.5	16
44	Methods for Inverting Dense Displacement Fields: Evaluation in Brain Image Registration. , 2007, 10, 900-907.		16
45	Consistency of parametric registration in serial MRI studies of brain tumor progression. International Journal of Computer Assisted Radiology and Surgery, 2008, 3, 201-211.	2.8	15
46	Neuroanatomical and Microglial Alterations in the Striatum of Levodopa-Treated, Dyskinetic Hemi-Parkinsonian Rats. Frontiers in Neuroscience, 2020, 14, 567222.	2.8	10
47	Shape and Texture. , 0, , 559-579.		9
48	Magnetic resonance imaging and tensor-based morphometry in the MPTP non-human primate model of Parkinson's disease. PLoS ONE, 2017, 12, e0180733.	2.5	9
49	X-Ray Mammogram Registration: A Novel Validation Method. Lecture Notes in Computer Science, 2006, , 197-204.	1.3	7
50	<title>Rate-equation analysis of Protoporphyrin IX photo-oxidation</title> ., 1996, , .		6
51	Biomechanical simulation of atrophy in MR images. , 2003, , .		5
52	Tracking displacements of intracellular organelles in response to nanomechanical forces. , 2008, , .		5
53	Accuracy Assessment of Global and Local Atrophy Measurement Techniques with Realistic Simulated Longitudinal Data. , 2007, 10, 785-792.		5
54	An Inverse Problem Approach to the Estimation of Volume Change. Lecture Notes in Computer Science, 2005, 8, 616-623.	1.3	4

WILLIAM R CRUM

#	Article	IF	CITATIONS
55	Simulation of Local and Global Atrophy in Alzheimer's Disease Studies. Lecture Notes in Computer Science, 2006, 9, 937-945.	1.3	4
56	Modelling Tumour Growth Patterns with Non-Rigid Image Registration. , 2007, , 139-144.		3
57	Fusion of rat brain histology and MRI using weighted multi-image mutual information. , 2008, , .		2
58	Magnetic Resonance Brain Image Processing and Arithmetic with FSL. Methods in Molecular Biology, 2011, 711, 109-126.	0.9	2
59	Spectral Clustering as a Diagnostic Tool in Cross-Sectional MR Studies: An Application to Mild Dementia. Lecture Notes in Computer Science, 2008, 11, 442-449.	1.3	1
60	<title>Measurement and modelling of protoporphyrin IX photo-oxidation during superficial PDT</title> . , 1996, , .		0
61	Patterns of cerebral atrophy in Alzheimer's disease and semantic dementia: A comparison of voxel based morphometry and region of interest measurements. NeuroImage, 2001, 13, 317.	4.2	0
62	Reply to: Lithium and the Expanding Brain. Biological Psychiatry, 2012, 72, e19.	1.3	0